Inorganic Chemistry

Open Access
This article is licensed under CC-BY 4.0

pubs.acs.org/IC
Article

Liquid Ammonia: More than an Innocent Solvent for Zintl Anions

Stefanie Gärtner, Michael Witzmann, Corinna Lorenz-Fuchs, Ruth M. Gschwind, and Nikolaus Korber*

Cite This: https://doi.org/10.1021/acs.inorgchem.4c01817
Read Online

ACCESS | Metrics & More | Article Recommendations | Supporting Information

ABSTRACT: Liquid ammonia as the original solvent for Zintl anions has been replaced by easier to handle or more versatile solvents in most recent Zintl chemistry. However, methodological advances have made it possible to structurally investigate the anions in ammoniate crystals via crystallography or in the solutions themselves via nuclear magnetic resonance. While in some cases liquid ammonia acts as an innocent solvent, it also provides different possibilities of direct involvement in chemical reactions. In addition to simple dissolution without changes to the anions observed in the solid starting materials, protonation of the anion, incongruent dissolution involving redox processes, and further oxidation and reduction products have been observed. The use of the solvent liquid ammonia under ambient pressure is limited to low temperatures, which in turn allows the monitoring of kinetically stabilized species, some of which cannot be accessed at higher temperatures. In this work, the available literature reports are summarized or referenced, and compounds that have been characterized as new ammoniate crystals are presented and contextualized. Innocent dissolution is observed for clusters involved in $K_{2.9}Rb_{5.1}[Si_4][Si_9]\cdot 15NH_3$, $Cs_4Sn_9\cdot 12NH_3$, $Cs_4Pb_9\cdot 5NH_3$, and $[Rb@[18]crown\text{-}6]_2[Rb@[2.2.2]crypt]Rb[Ge_9]\cdot 4NH_3$. Formal protonation of $[Ge_4]^{4-}$ results in the crystallization of $[Na@[2.2.2]crypt]_2[H_2Ge_4]\cdot 3NH_3$. Tt_5^{2-} (Tt = Sn or Pb) and HSi_9^{3-} cannot be accessed in a binary solid state material but can be crystallized in co-crystals of PPh_3 in $[Rb@[2.2.2]crypt]_2[Sn_5][PPh_3]_2\cdot NH_3$, $[Rb@[2.2.2]crypt]_2[Pb_5][PPh_3]_2\cdot NH_3$, and $[K@[2.2.2]crypt]_3[HSi_9][PPh_3]\cdot 5NH_3$.

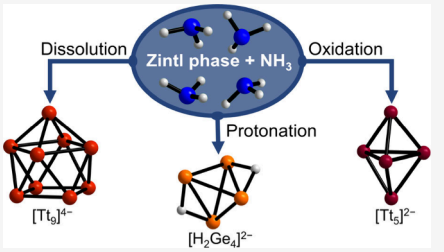

Downloaded via UNIV REGENSBURG on August 14, 2024 at 09:47:57 (UTC).
See https://pubs.acs.org/sharingguidelines for options on how to legitimately share published articles.

INTRODUCTION

In 1891, A. Joannis reported on a green solution derived by the simultaneous dissolution of sodium metal and elemental lead in liquid ammonia.[1] Although not being interpreted as such, this observation is the first documented evidence of a homoatomic polyanion of a main group metal produced in solution. Four decades later, E. Zintl produced and first structurally characterized the Zintl phase NaTl by reducing thallium(I) iodide in a solution of sodium in liquid ammonia.[2,3] Again four decades later, Kummer and Diehl changed the solvent to ethylenediamine[4] and Corbett introduced cryptand as a sequestering agent and reported the first clear crystal structure of a Zintl ion of a group 14 metal obtained by dissolution experiments.[4,5] Although single crystals in liquid ammonia had been observed visually, these alterations were necessary for structural elucidation as X-ray structure analysis at that time was not possible for thermally labile crystals. Today, standard preparation techniques for labile crystals are applied widely for sensitive compounds and are used in all branches using this analytical method. In particular, the development of low-temperature devices and procedures allows for investigations of solvate crystals that decompose well below room temperature. For Zintl chemistry, this opened the door for investigation of very sensitive single crystals. In the following, we concentrate on the solvent with which everything had started, liquid ammonia. Upon closer examination of the reported species derived by (re)crystallization experiments in this solvent, it becomes evident that liquid ammonia might act as an innocent solvent but provides the capabilities of taking part in different reactions. In 1985, J. D. Corbett, to whom we owe major advances in the field of Zintl chemistry, stated, "The dependence of results on solvent has generally not been well explored."[6] In the past decades, a number of versatile compounds, which were obtained by various dissolution experiments and reactions, have been reported in review articles.[7−15] The products are often unpredicted and surprising and emphasize the role of Zintl anions as a key to new homoatomic bonding motifs and interesting reactivities.[8,10,16−20] The scope of this article is not to illustrate these well-reported issues. In contrast, we here go back to the roots and address a very general question. What reactivities of Zintl anions can be expected in solvent liquid ammonia? To obtain homoatomic p-block (semi)metal clusters in solution, there are different Zintl phases available. In general, the solubility of these materials in liquid ammonia is limited to compounds including alkali metals as less electronegative constituents. For group 14, A_4Tt_4 (A = Na−Cs, and Tt = Si−Pb),[21−29] A_4Tt_9 (A = Na−Cs, and Tt = Ge−Pb),[30−33] and $A_{12}Tt_{17}$ (A = Na−Cs, and Tt = Si−Pb)[32,34] are generally used,

Special Issue: Dialogue on Zintl Chemistry

Received: May 2, 2024
Revised: July 24, 2024
Accepted: July 26, 2024

ACS Publications
© XXXX The Authors. Published by American Chemical Society

https://doi.org/10.1021/acs.inorgchem.4c01817
Inorg. Chem. XXXX, XXX, XXX−XXX

while the solubility for silicides is commonly known to be best for $A_{12}Si_{17}$ materials.[35−38] In accord with the Zintl−Klemm concept, these materials include tetrahedral $[Tt_4]^{4-}$ and/or monocapped square antiprismati- shaped $[Tt_9]^{4-}$ polyanions. $A_{12}Tt_{17}$ contains $[Tt_9]^{4-}$ and $[Tt_4]^{4-}$ clusters in a 1:2 ratio. For stannides, additionally $A_{52}Sn_{82}$ (A = K or Cs) is known, which also involves $[Sn_4]^{4-}$ and $[Sn_9]^{4-}$ clusters.[39] It has to be noted that especially the materials of the heavier tetrelides suffer from low crystallinity due to disorder and the formation of plastic crystalline phases.[40,41] Convenient representatives for dissolution experiments of group 15 Zintl phases are A_3Pn_7 (A = Na−Cs, and Pn = P−Sb),[42−47] A_3Pn_{11} (A = Na−Cs, and Pn = P−Sb),[48−50] and A_4Pn_6 (A = Rb or Cs, and Pn = P or As).[51−53] The A_3Pn_7 phases contain nortricyclane-shaped $[Pn_7]^{3-}$ clusters and the A_3Pn_{11} phases tris-homocubane-shaped $[Pn_{11}]^{3-}$ (ufosan). In A_4Pn_6 planar, non-aromatic $[Pn_6]^{4-}$ anions[54] represent the anionic entity.

The dissolution route uses the soluble Zintl phases mentioned above of the alkali metals, which are prepared by classical solid state methods and subsequently dissolved in liquid ammonia.[55] The anions detected in the ammoniate crystals that precipitate allow conclusions to be drawn about the species present in the solution. It has to be pointed out that while detecting a Zintl anion in an ammoniate crystal is a very strong indication that it has been present in solution, this does not per se preclude the presence of additional different species or even rearrangements during the process of crystallization. Unfortunately, additional analytical methods are very difficult to apply due to the solvent being a condensed medium only below −33 °C at ambient pressure. Higher temperatures directly cause spontaneous vaporization. In this context, E. Zintl's very accomplished experimental works have to be emphasized, as he performed potentiometric titrations in this solvent many decades ago.[3] In recent years, attempts have succeeded in preparing nuclear magnetic resonance (NMR) probes for low-temperature measurements. Standard NMR probes with the coil for broadband detection located either as the inner or the outer coil provide large temperature ranges compatible with the requirements for liquid ammonia as the solvent and had been successfully applied in Zintl anion detection.[56,57] The sensitivity of these probes is limited, but the large temperature range allows even for temperature-dependent studies down to 180 K. In contrast, the newer probes with cryogen-cooled coils provide excellent sensitivities for low-concentration species or slowly reacting ions.[58,59]

However, these cryoprobes have a reduced temperature range of ∼80 °C limiting low-temperature measurements to ≥240 K. These probes can be used only for elements for which NMR active isotopes are available. For homoatomic Zintl anion chemistry investigations in liquid ammonia solutions, ^{31}P,[54,60] ^{29}Si,[36,56,57] and ^{119}Sn[36,61] have been reported. Very recently, the possibility of detecting Raman spectra from ammoniate crystals in bomb tubes was shown,[62] which might also be applicable for Zintl cluster ammoniates in the future. At the moment, information about ongoing processes during dissolution is based on solvate crystal structures and solution NMR spectroscopy where available. In the following, we provide an overview of the observed species during dissolution experiments of alkali metal tetrelides (Tt) and pnictogenides (Pn) in a liquid ammonia solution and new compounds $K_{2.9}Rb_{5.1}[Si_4][Si_9]\cdot 15NH_3$ (**1**), $Cs_4Sn_9\cdot 12NH_3$ (**2**), $Cs_4Pb_9\cdot 5NH_3$, (**3**) $[Rb@[18]crown\text{-}6]_2[Rb@[2.2.2.]crypt]Rb[Ge_9]\cdot 4NH_3$ (**4**), $[Na@[2.2.2]crypt]_2[H_2Ge_4]\cdot 3NH_3$ (**5**), $[Rb@[2.2.2]crypt]_2[Sn_5][PPh_3]_2\cdot NH_3$ (**6**), $[Rb@[2.2.2]crypt]_2[Pb_5][PPh_3]_2\cdot NH_3$ (**7**), and $[K@[2.2.2]crypt]_3[HSi_9][PPh_3]\cdot 5NH_3$ (**8**) are contextualized.

MATERIALS AND METHODS

Synthesis. *$K_{2.9}Rb_{5.1}[Si_4][Si_9]\cdot 15NH_3$ (**1**).* First, 30 mg (0.025 mmol) of the solid state material with the nominal composition $K_6Rb_6Si_{17}$ and 13 mg (0.013 mmol) of dibenzo-[18]crown-6 were dissolved in 5 mL of anhydrous liquid ammonia. The reddish orange solution was stored for nine months at 203 K, and orange needles of **1** could be isolated and characterized by single-crystal X-ray diffraction (SCXRD).

*$Cs_4Sn_9\cdot 12NH_3$ (**2**).* First, 200 mg (0.125 mmol) of the solid state material with the nominal composition Cs_4Sn_9 was dissolved in 5 mL of anhydrous liquid ammonia. The dark red solution was stored for five months at 203 K, and red crystals of **1** could be isolated and characterized by SCXRD. In addition, a solution of 200 mg of the nominal phase Cs_4Sn_4 in 5 mL of anhydrous liquid ammonia yielded crystals of **2** after storage at 203 K for five months.

*$Cs_4Pb_9\cdot 5NH_3$ (**3**).* First, 211 mg (0.848 mmol) of cesium, 389 mg (1.878 mmol) of lead, and 55 mg (0.207 mmol) of [18]crown-6 were dissolved in anhydrous liquid ammonia. After storage at 233 K for two months, black blocks of **3** could be isolated and characterized by SCXRD.

*$[Rb([18]crown\text{-}6)]_2[Rb@[2.2.2]crypt]Rb[Ge_9]\cdot 4NH_3$ (**4**).* First, 50 mg (0.022 mmol) of the solid state material with the nominal composition $Rb_{12}Ge_{17}$ and 12.4 mg (0.033 mmol) of [2.2.2]crypt were dissolved in anhydrous liquid ammonia, yielding a reddish brown solution. After storage at 203 K for four months, yellow needles of **4** could be isolated and characterized by SCXRD.

*$[Na@[2.2.2]crypt]_2[H_2Ge_4]\cdot 3NH_3$ (**5**).* First, 50 mg (0.022 mmol) of the solid state material with the nominal composition $Rb_{12}Ge_{17}$, 22 mg (0.083 mmol) of [18]crown-6, and 19 mg (0.049 mmol) of [2.2.2]crypt were dissolved in anhydrous liquid ammonia, yielding a yellow solution. After storage at 203 K for four months, yellow crystals of **5** could be isolated and characterized by SCXRD.

*$[Rb@[2.2.2]crypt]_2[Sn_5][PPh_3]_2\cdot NH_3$ (**6**).* First, 25 mg (0.030 mg) of the solid state material with the nominal composition Rb_4Sn_4, 12 mg (0.030 mmol) of [2.2.2]crypt, and 35 mg (0.030 mmol) of $Pd(PPh_3)_4$ were dissolved in anhydrous liquid ammonia. After storage at 233 K for six months, dark red blocks of **6** could be isolated and characterized by SCXRD.

*$[Rb@[2.2.2]crypt]_2[Pb_5][PPh_3]_2\cdot NH_3$ (**7**).* First, 50 mg (0.040 mmol) of the solid state material with the nominal composition Rb_4Pb_4, 24.1 mg (0.060 mmol) of [2.2.2]crypt, and 21.1 mg (0.040 mmol) of $Au(PPh_3)Cl$ were dissolved in anhydrous liquid ammonia, yielding a dark green solution. After storage at 233 K for two months, dark violet plates of **7** could be isolated and characterized by SCXRD.

*$[K@[2.2.2]crypt]_3[HSi_9][PPh_3]\cdot 5NH_3$ (**8**).* First, 30 mg (0.025 mmol) of the solid state material with the nominal composition $K_6Rb_6Si_{17}$, 28 mg (0.073 mmol) of [2.2.2]crypt, 9 mg (0.037 mmol) of [18]crown-6, and 30 mg (0.025 mmol) of $Pt(PPh_3)_4$ were dissolved in anhydrous liquid ammonia, yielding an orange brown solution. After storage at 233 K for one year, yellow blocks of **8** could be isolated and characterized by SCXRD.

Single-Crystal X-ray Diffraction. For the general procedure, see the Supporting Information for details regarding the individual compounds. All compounds are highly sensitive to moisture, air, and temperature. A small amount of crystals was transferred directly from the mother liquor from a cooled Schlenk vessel into liquid nitrogen stream-cooled perfluoroether oil. Suitable single crystals were isolated and subsequently transferred onto the goniometer using a MiTeGen loop cooled in liquid nitrogen during the transport. Data were collected at a temperature of 123 K with different diffractometers (see the Supporting Information for the respective setup used for the individual compounds). For data reduction, CrysAlisPro was used. Structure solution (ShelXT)[63] and refinement (ShelXL)[64] were performed in Olex2.[65] The figures were created in Diamond 4[66] using displacement ellipsoids at the 50% probability level.

https://doi.org/10.1021/acs.inorgchem.4c01817
Inorg. Chem. XXXX, XXX, XXX−XXX

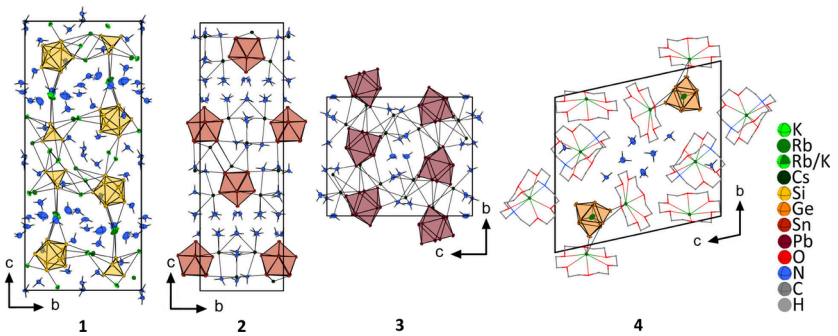

Figure 1. Unit cells of $K_{2.9}Rb_{5.1}[Si_4][Si_9]\cdot 5NH_3$ (**1**), $Cs_4Sn_9\cdot 12NH_3$ (**2**), $Cs_4Pb_9\cdot 5NH_3$ (**3**), and $[Rb@[18]crown\text{-}6]_2[Rb@[2.2.2]crypt]Rb[Ge_9]\cdot 5NH_3$ (**4**). For the sake of clarity, disorder and A−N (A = K or Rb) contacts in **1** have been omitted (for details, see Figure S2), whereas chelating agents in **4** are shown as wires and sticks.

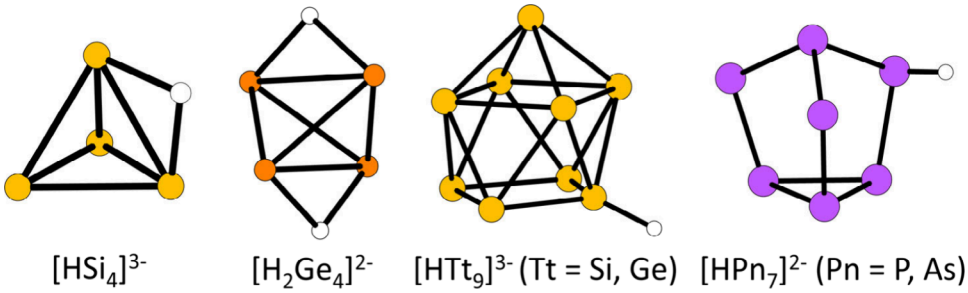

Figure 2. Overview of some of the known protonated tetrelides (Tt) and pnictogenides (Pn) from liquid ammonia.

Table 1. Protonated Tetrelide Clusters in Liquid Ammonia

cluster	method or compound	ref
$[HSi_4]^{3-}$	^{29}Si NMR	57
$[H_2Ge_4]^{2-}$	$[Na(crypt)]_2[H_2Ge_4]\cdot 3NH_3$	this work
$[HTt_9]^{3-}$	$(K(DB\text{-}[18]crown\text{-}6))(K@[2.2.2]crypt)_2[HSi_9]\cdot 8.5NH_3$	56
Tt = Si or Ge	$[Rb@crypt]_2[Rb([18]crown\text{-}6)][HGe_9]\cdot 4NH_3$	96
	$[K([18]crown\text{-}6)_3(HSi_9)]\cdot 2NH_3\cdot 2THF$[a]	95

[a]After dilution with tetrahydrofuran and exchange of NH_3.

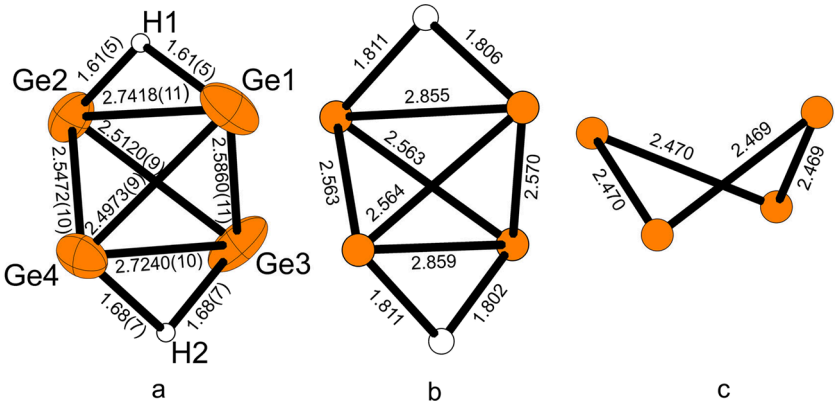

Figure 3. Atom arrangement and distances in $[H_2Ge_4]^{2-}$ (a) from the crystal structure and (b) for an optimized geometry. (c) Optimized geometry of a hypothetical $[Ge_4]^{2-}$.

RESULTS AND DISCUSSION

Dissolution without Reaction. The simplest process of generating Zintl anions in solution is represented by the dissolution of Zintl phases, including precast polyanions, where no subsequent reaction of the anions is monitored. The solubility of the Zintl salts can be influenced by applying different sequestering agents. For this reason, [18]crown-6 (1,4,7,10,13,16-hexaoxacyclooctadecane) or [2.2.2]cryptand (4,7,13,16,21,24-hexaoxa-1,10-diazabicyclo[8.8.8]hexacosane) is commonly used. The cryptates in return also facilitate crystallization, and these large molecular units significantly influence the observed three-dimensional structure in the solid state. Ammonia molecules of crystallization can act as rather innocent additives concerning solid state structures. Already in

https://doi.org/10.1021/acs.inorgchem.4c01817
Inorg. Chem. XXXX, XXX, XXX−XXX

Table 2. Unit Cell Parameters of $(A@[2.2.2]crypt)_2Tt_5$ and Related Compounds That Suggest Similar Three-Dimensional Arrangements

	X_2Sn_5[104],[a]	X_2Pb_5[105],[a]	$X_2[H_2Ge_4]\cdot 3NH_3$[a]	$Z_2Ge_5\cdot 4NH_3$[106],[b]
a (Å)	11.620(1)	11.615(3)	11.6200(6)	11.2887(9)
b (Å)	11.620(1)	11.615(3)	21.8720(7)	11.8949(9)
c (Å)	22.160(7)	22.120(12)	11.6979(6)	11.9433(9)
α (deg)	90	90	90	117.911(8)
β (deg)	90	90	119.469(6)	98.650(9)
γ (deg)	120	120	90	91.797(9)
crystal system, space group	trigonal, $P3c1$	trigonal, $P\bar{3}c1$	monoclinic, $P2_1$	triclinic, $P1$

[a]For the sake of clarity, the cryptand complexes have been replaced by X = (Na@[2.2.2]crypt). [b]For the sake of clarity, the cryptand complexes have been replaced by Z = (K@[2.2.2]crypt).

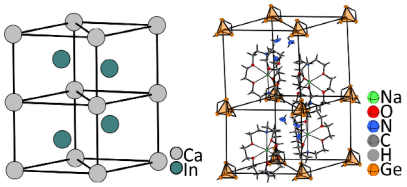

Figure 4. Structural similarity of $CaIn_2$ and $[Na@[2.2.2]\text{-}crypt]_2[H_2Ge_4]\cdot 3NH_3$.

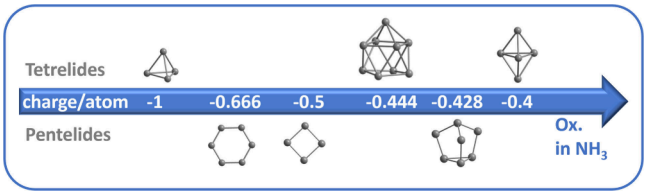

Figure 5. Clusters in tetrelide and pnictogenide Zintl phases in the dependency of charge per atom. Highly reduced clusters like $[Tt_4]^{4-}$ and $[Pn_6]^{4-}$ tend to dissolve incongruently, while the less reduced species like $[Tt_9]^{4-}$ or $[Pn_7]^{3-}$ are found to be stable in liquid ammonia solution.

1989, the room-temperature stable ammoniate $Cs_3(NH_3)As_7$ was prepared and the comparison to Cs_3As_7 demonstrated the possibility of including ammonia of crystallization in binary Zintl phases.[67] The obtained ammoniate is structurally related to the parental phase Cs_3As_7. A similar observation can be deduced for group 14 by comparing A_4Tt_4 (A = alkali metal, and Tt = Si−Pb) solid state phases and ammoniate structures.[68] The first coordination sphere of the anion in the binaries and ammoniates is strongly related. Subsequently, several "pure" ammoniate crystal structures without further additives of $[Tt_9]^{4-}$, $[Tt_4]^{4-}$, $[Pn_7]^{3-}$, and $[Pn_{11}]^{3-}$ have been reported, all of which prove the innocent dissolution of the parental phases in liquid ammonia. In addition, it could be shown that $[As_6]^{4-}$ rings are retained in solution when dissolving binary phase Rb_4As_6.[60] Heavier alkali metal cations K^+−Cs^+ tend to coordinate directly to the cluster units; therefore, usually three-dimensional cation−anion networks are observed. An example is given by $K_{2.9}Rb_{5.1}[Si_4][Si_9]\cdot 15NH_3$ [**1** (Figure 1); for crystallographic information, see Table S1], which could be crystallized from solutions of silicide $K_6Rb_6Si_{17}$ in liquid ammonia. The compound is structurally related to $K_8[Si_4][Si_9]\cdot 14.6NH_3$[69] and demonstrates the possibility of substituting two potassium positions by rubidium (see Figure S1), while the remaining alkali cation sites are mixed occupied by potassium and rubidium.

In general, ammonia acting as a ligand toward the alkali cations is also capable of breaking the three-dimensional cation−anion network. This is usually the case when lithium or sodium is present, as homoleptic ammine complexes are formed. For example, in $[Li(NH_3)_4]_3As_7\cdot NH_3$ or $[Li(NH_3)_4]_4Sn_9\cdot NH_3$ and $[Li(NH_3)_4]_4Pb_9\cdot NH_3$ lithium−tetraammine complexes are present, which prevent direct cation−anion contacts.[70,71] In contrast, $Cs_4Sn_9\cdot 12NH_3$ (**2**) represents a new and first example in which the high ammonia content causes the formation of Cs^+−$[Sn_9]^{4-}$ double layers built from cation−anion interactions, which are separated by ammonia molecules only [**2** (Figure 1); for crystallographic information, see Table S3]. To date, the formation of these types of layers in the respective crystal structures was observed only when cryptates or crown ethers were present during crystallization. Thus, $Cs_4Sn_9\cdot 12NH_3$ shows the broad variety of possible arrangements in ammoniate crystal structures, even in the

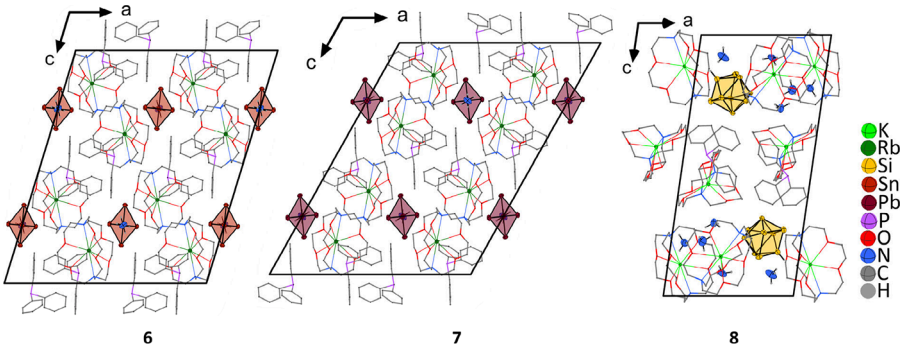

Figure 6. Projection of the unit cells of the compounds $[Rb@[2.2.2]crypt]_2[Sn_5][PPh_3]_2\cdot NH_3$ (**6**), $[Rb@[2.2.2]crypt]_2[Pb_5][PPh_3]_2\cdot NH_3$ (**7**), and $[K@[2.2.2]crypt]_3[HSi_9][PPh_3]\cdot 5NH_3$ (**8**) along the crystallographic b-axis. For the sake of clarity, [2.2.2]crypt and PPh_3 are shown as wires and sticks.

https://doi.org/10.1021/acs.inorgchem.4c01817
Inorg. Chem. XXXX, XXX, XXX−XXX

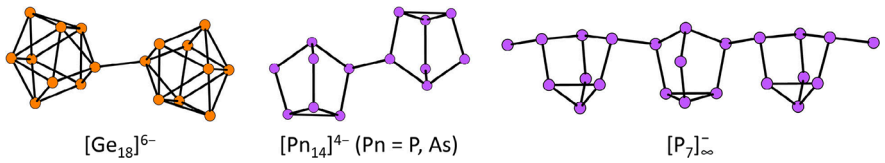

Figure 7. Overview of selected condensed tetrelide or pnictogenide clusters from liquid ammonia. A detailed overview for groups 14 and 15 is given in refs 14 and 18.

simplest case without additives. This is underlined by the crystal structure of $Cs_4Pb_9{\cdot}5NH_3$ (**3**), which indeed shows the expected three-dimensional cation−anion network [**3** (Figure 1); for crystallographic information, see Table S5]. As mentioned above, the addition of cryptating agents prevents the formation of a three-dimensional network. This is also well-reported for tetrelide cluster solvates of the solvent ethylenediamine.[8] The same is true in liquid ammonia,[38,70,72] and in the new example, [Rb@[18]crown-6]$_2$[Rb@[2.2.2]crypt]Rb-[Ge_9]·4NH_3 (**4**), the coordination motifs for Rb^+ can be nicely demonstrated, as [Rb@[18]crown-6]$^+$, [Rb@2.2.2crypt]$^+$, and nonchelated Rb^+ are present in the unit cell [**4** (Figure 1); for crystallographic information, see Table S7].

Altogether, recrystallization experiments suggest a certain stability of the precast $[Tt_9]^{4-}$, $[Pn_7]^{3-}$, and $[Pn_{11}]^{3-}$ anions in solution. This is also supported by ^{119}Sn NMR of binary stannides in liquid ammonia. The $[Sn_9]^{4-}$ clusters are not affected by the solvent, as the well-known signal at approximately −1200 ppm is stable for a long time under these solutions.[61] In contrast, the availability of $[Sn_4]^{4-}$ clusters in solutions of Rb_4Sn_4 can be monitored by its characteristic ^{119}Sn signal at approximately −1800 ppm, which is observed only when cryptand is added or when the stannides are produced by an experimental procedure different from dissolution (direct reduction). This can be interpreted as a first hint that these clusters provide additional reactivities in a liquid ammonia solution. In general, ammoniate crystals of the ligand-free tetrahedral $[Tt_4]^{4-}$ clusters are rarely observed compared to the comparatively stable $[Tt_9]^{4-}$.[35,68,73,74]

Reactions in and/or with Liquid Ammonia. The oxidation of Zintl phases is a chemically plausible and straightforward way to form bonds and the buildup of larger homoatomic entities, and different groups address this issue by various approaches under a range of experimental conditions.[75−80] In particular, the oxidative coupling of homoatomic polyanions to form new elemental modifications is very promising.[81−83] A prominent example is the oxidation of homoatomic clusters $[Ge_9]^{4-}$ in ionic liquids, as even a new elemental modification of germanium in terms of a guest-free germanium clathrate could be achieved.[84] Furthermore, a variety of other novel mesoporous germanium materials can be obtained through the oxidation of such anionic clusters.[85−87] Another example, which involves alkali metal Zintl phases, including cluster units, is the oxidation of K_4Si_4 under hydrogen pressure. There, reversible oxidation produces $KSiH_3$, which is thus discussed as a promising material for hydrogen storage.[88] The reactions with liquid ammonia at low temperatures allow the isolation of kinetically stabilized transitional compounds and therefore can yield precious information about ongoing processes during oxidation reactions. In general, one must distinguish among three reaction pathways. First, the clusters are in equilibrium with their oxidized counterparts and solvated electrons.[89] Second, protonation of the clusters is possible due to the protic character of the solvent liquid ammonia (Protonation). Finally, incongruent dissolution can be observed for some Zintl phases, which yields new or formally oxidized homoatomic polyanions (Incongruent Dissolution). Different additives allow for the formation of interlinked clusters, the combination of both reaction pathways, or co-crystal formation (Further Examples of Oxidations and Reactions).

Protonation. Phosphorus hydrides including protonated Zintl clusters have thoroughly been studied by ^{31}P NMR in different solvents.[90−93] Additionally, HSn_9^{3-}[94] and $H_2Si_9^{2-}$[95] in different solvents are reported in the literature. In liquid ammonia, protonation of homoatomic Zintl anions is known for silicon, germanium, phosphorus, and arsenic by single-crystal X-ray structures and/or solution NMR investigations. It has to be noted that protonation of the anion in this context is the formal reaction only. According to the electronegativities, the H atom in the protonated anion has to be considered as hydride, which is supported by the chemical shifts in related ^{1}H NMR investigations.[56,57,91,94] The Brønsted acid−base chemistry of pnictogenide clusters is discussed and summarized elsewhere;[13,14] therefore, the focus here is set on the tetrelide clusters. Figure 2 shows examples for protonated tetrelide and pnictogenide clusters obtained from liquid ammonia solutions, and Table 1 gives examples for protonated tetrelides in and/or from liquid ammonia.

In general, the observation of protonated clusters in liquid ammonia seems to be restricted to the lighter homologues of a group, which is in accord with the rapidly decreasing stability of the element hydrides of the heavier congeners. While the ^{31}P NMR investigations of M. Baudler mentioned above proved the formation of protonated phosphide clusters by the reduction of diphosphane in liquid ammonia,[90] single crystals of the latter from liquid ammonia solutions were observed only when additives were present.[97−99] In contrast, the protonation of silicides occurs spontaneously without the need for further additives. This is plausible given the higher charge of the tetrelides.

Attention needs to be drawn to protonated tetrahedral $[Tt_4]^{4-}$ species. While $[HSi_4]^{3-}$ was unambiguously detected in ^{29}Si NMR experiments, a related crystal structure involving this anion is still missing. Interestingly, it was shown by the single-crystal structure of [K@[18]crown-6][Rb@[18]crown-6]$_2$[HGe_4ZnPh_2]·8NH_3[100] that the related $[HGe_4]^{3-}$ can act as a ligand toward transition metals. To the best of our knowledge, similar observations of $[HSi_4]^{3-}$ are still missing. ^{29}Si NMR solution studies and subsequent theoretical calculations suggest the protonation taking place not at one vertex of the tetrahedron but edge capping,[57] just as in the heavier congener $[HGe_4]^{3-}$ in $[HGe_4ZnPh_2]^{2-}$. This is also supported by calculations dealing with the solid state material K_2BaSi_4,[101] which also suggest that the protonation of one vertex of $[Si_4]^{4-}$ is less favored. This is also observed for valence isoelectronic $[HP_4]^+$ cation with edge-capping hydrogen, according to the pseudoelement concept.[102,103] Crystal-

https://doi.org/10.1021/acs.inorgchem.4c01817
Inorg. Chem. XXXX, XXX, XXX−XXX

lization of ligand-free protonated tetrelides is very rarely observed. We recently succeeded in crystallizing $[Na@[2.2.2]\text{-crypt}]_2[H_2Ge_4]\cdot 3NH_3$, which includes $[H_2Ge_4]^{2-}$ anions. Unfortunately, the quality of the diffraction data of the SCXRD experiment is insufficient for determining the positions of the H atoms, which therefore have been modeled in the refinement using restraints. The positions of the Ge atoms yield distances that differ significantly from those of an ideal $[Ge_4]^{4-}$ tetrahedron (2.5−2.6 Å)[68] as two edges are elongated (2.7418(11) and 2.7240(11) Å), which supports the structural interpretation. A first geometry optimization also strongly indicates a protonated species, as the optimized geometry for unprotonated $[Ge_4]^{2-}$ did not result in a tetrahedral anion but a strongly distorted four-atom ring. In contrast, the obtained Ge−Ge distances of the optimized geometry for $[H_2Ge_4]^{2-}$ match the experimental values from the crystal structure very well (Figure 3; for computational details and crystallographic information see Table S9). Therefore, the overall charge of −2 together with the best structure solution from single-crystal data of the proposed model strongly supports the presence of $[H_2Ge_4]^{2-}$ in liquid ammonia.

Upon closer examination of the unit cell parameters of $[Na@[2.2.2]crypt]_2[H_2Ge_4]\cdot 3NH_3$, a relationship with the $(A@[2.2.2]crypt)_2Tt_5$ compounds (Tt = Sn or Pb)[5,104,105] that contain E_5^{2-} anions becomes evident (Table 2).

While the ammonia-free compounds crystallize in high-symmetry trigonal space groups $P3c1$ and $P\bar{3}c1$, respectively, ammonia of crystallization causes a lower observed symmetry. The cell parameters of $[Na@[2.2.2]crypt]_2[H_2Ge_4]\cdot 3NH_3$ still resemble a trigonal metric of the unit cell; in contrast, the symmetry in $[K@[2.2.2]crypt]_2Ge_5\cdot 4NH_3$ is reduced even to triclinic $P1$ without any additional translational symmetry except identity.[106]

In general, these compounds can be structurally related to binary $CaIn_2$,[104] and ammonia of crystallization causes a distortion in that arrangement in $[A@[2.2.2]crypt]_2Tt_5\cdot 4NH_3$ (Tt = Si or Ge).[37] A similar structural relationship can be visualized for $[Na@[2.2.2]crypt]_2[H_2Ge_4]\cdot 3NH_3$ (Figure 4). Of course, the atom positions differ significantly, which makes a comparison in terms of a formal isostructural derivation impossible.

The 2-fold negatively charged anion governs the 1:2 anion:cryptand ratio, which results in the best three-dimensional arrangement in the (distorted) $CaIn_2$ packing. This is true for $[Tt_5]^{2-}$ (Tt = Si−Pb) as well as for $[H_2Ge_4]^{2-}$ and demonstrates that for the evaluation of the observable anions in the solid state by recrystallization experiments the optimized packing in three dimensions should not be neglected.

Incongruent Dissolution. The central challenge for the clean generation of Zintl ions in solution from solid state starting materials is posed by the reactivity toward the solvent. In the case of liquid ammonia, the clusters mentioned in Protonation can be readily dissolved and (re)crystallized as ammoniates from the solutions, which indicates that they are at least somewhat stable toward this traditional Zintl ion solvent. In contrast, incongruent dissolution is also possible and common where the precast entity in the solid state transforms during dissolution. In these cases, mainly formally oxidized molecular units can be observed. With regard to group 14, incongruent dissolution is observed in NMR experiments for Rb_4Sn_4, which leads to $[Sn_9]^{4-}$ cage anions in the liquid ammonia solutions.[61] Further evidence for this transformation from $[Sn_4]^{4-}$ to $[Sn_9]^{4-}$ is provided by the fact that $Cs_4Sn_9\cdot 12NH_3$ (**2**) could also be crystallized from cryptand-free solutions of Cs_4Sn_4 (see Materials and Methods for **2**). In contrast, upon addition of [2.2.2]crypt, $[Sn_4]^{4-}$ anions can be detected as they accumulate and are stabilized in solution. The presence of [2.2.2]crypt in return enables the crystallization of trigonal bipyramidal-shaped $[Sn_5]^{2-}$ anions,[104,105,107] for which no binary solid state material is known. The same is true for $[Pb_5]^{2-}$, which forms from solutions of Na_4Pb_4 and K_4Pb_4 in the presence of cryptand in liquid ammonia.[5,105] The large cryptate complexes enable crystallization of $[A@[2.2.2]\text{-crypt}]_2Tt_5$, which is hierarchically related to the $CaIn_2$ structure type (see above). The lighter homologues yield $[A@[2.2.2]crypt]_2Tt_5\cdot 4NH_3$ crystals from solutions of $A_{12}Tt_{17}$ materials (Tt = Si or Ge).[37,106,108] In the crystal structures of the latter, additional ammonia of crystallization is needed for effective packing in lower-symmetry triclinic space groups. While $[Tt_9]^{4-}$ clusters are known to be more or less flexible on the NMR time scale,[56,94,95] the ^{29}Si NMR signal of $[Si_5]^{2-}$ recently proved the rigid character of the trigonal bipyramidal-shaped anion.[57]

Even approximately 50 years ago, the use of cryptand also provided the possibility of observing Sb_4^{2-} and Bi_4^{2-} anions crystallizing from not further characterized metallic alloys upon dissolution in ethylenediamine.[109,110] The lighter homologues As_4^{2-} and P_4^{2-} can also be accessed by directly reducing red phosphorus or gray arsenic in liquid ammonia.[54,111−113] Furthermore, the dissolution of A_4Pn_6 (A = Rb or Cs, and Pn = P or As) does not result in $[P_6]^{4-}$ but yields lone-pair aromatic $[P_4]^{2-}$ anions as a formal oxidation product. $[As_6]^{4-}$ is known to be more stable in solution as ammoniate crystals that contain this anion have been obtained (see Protonation). Additionally, dissolution of A_4As_6 (A = Rb or Cs) also provides formally oxidized As_7^{3-}[70] and As_4^{2-}[54,111] in solution.

Very recently, it was shown that group 13 Zintl phases Na_2In and Na_7KIn_4 are oxidized upon dissolution in liquid ammonia to form binary NaIn. As Na_7KIn_4 includes tetrahedral Zintl anion $[In_4]^{8-}$, this might be interpreted as the first evidence for a solution behavior of trielides in anhydrous liquid ammonia similar to the reactivities of tetrelides or pnictogenides mentioned above.[114−116]

Altogether, Zintl phases including more reduced cluster species tend to dissolve incongruently under the formation of formally oxidized cluster units in solution (Figure 5). Simultaneously, ammonia is reduced to form alkali metal amide and elemental hydrogen. In general, the side product alkali metal amide can be detected by NMR in solution as well as by PXRD of the residue after the evaporation of ammonia.

Further Examples of Oxidations and Reactions. The examples mentioned above are due to reactions with ammonia as no further additives except [18]crown-6 or cryptand were added. In the past, attention was drawn to reactions of the cluster units with different transition metal complexes. This gave rise to further observations, because co-crystallization is possible with, e.g., PPh_3, as this well-known ligand molecule was present in solution due to the degradation of the complexes. In $[Rb@[2.2.2]crypt]_2[Sn_5][PPh_3]_2\cdot NH_3$ and $[Rb@[2.2.2]crypt]_2[Pb_5][PPh_3]_2\cdot NH_3$, PPh_3 is present in addition to the cryptates in the unit cells and obviously further facilitates the crystallization of $[Tt_5]^{2-}$ upon incongruent dissolution of the Zintl phases Rb_4Sn_4 and Rb_4Pb_4, respectively. This is also true for $[K@[2.2.2]crypt]_3[HSi_9]\text{-}[PPh_3]\cdot 5NH_3$, where the protonated silicide is present in the

https://doi.org/10.1021/acs.inorgchem.4c01817
Inorg. Chem. XXXX, XXX, XXX−XXX

unit cell (Figure 6; for crystallographic information about the compounds, see Tables S11, S13, and S15).

In contrast to $[Na@[2.2.2]crypt]_2[H_2Ge_4]\cdot 3NH_3$, in $[Rb@[2.2.2]crypt]_2[Sn_5][PPh_3]_2\cdot NH_3$ and $[Rb@[2.2.2]\text{-}crypt]_2[Pb_5][PPh_3]_2\cdot NH_3$ the additive PPh_3 causes an even more distorted structure that cannot be directly related to $CaIn_2$ (for further information, see Figure S10). More systematic investigations of crystal packing in co-crystals with further additives like PPh_3 could show if up to now hidden Zintl ions might be accessible in co-crystals.

More severe conditions are necessary to observe the oxidative coupling of group 14 and group 15 clusters to form larger interlinked clusters, as these are obtained exclusively when additional oxidants are provided. The oxidative strength of the solvent liquid ammonia itself seems not to be sufficient for the formation of interlinked clusters like, e.g., $[P_{14}]^{4-}$[117] or $[Ge_{18}]^{6-}$[118] (Figure 7).

The observations of these units from liquid ammonia solution are very serendipitous and are not yet well understood. A very rare example is represented by CsP_7, which is formed by the reaction of Cs_3P_{11} and tellurium in liquid ammonia. CsP_7 includes one-dimensional chains of linked P_7 clusters, but no ammonia molecules of crystallization are present.[119] This example emphasizes the large potential of liquid ammonia also for preparing binary compounds and alloys, which are difficult to access by classical solid state synthesis.

SUMMARY

Zintl anions in liquid ammonia make up a very fascinating and at the same time very challenging class of compounds, as their chemistry in solution is dependent on a filigree interplay of stabilization in solid state, solubility, and acidity. The documentation of results, obtained by crystallization and NMR in solution, allows one to gain further insights into ongoing processes. Slight changes in the experimental approach often result in a severe impact on the whole system. The results demonstrate that the common hypothesis of liquid ammonia as not only a historic but also a prototypic innocent solvent for Zintl anions needs to be revised. In other words, liquid ammonia must also be seen as a very potent reaction medium for yet not very well investigated ongoing oxidation processes of Zintl anions at low temperatures.

ASSOCIATED CONTENT

Supporting Information

The Supporting Information is available free of charge at https://pubs.acs.org/doi/10.1021/acs.inorgchem.4c01817.

Computational details, additional synthetic details, crystallographic information and selected interatomic distances for all compounds, and structural comparison of **5**–**7** with $CaIn_2$ (PDF)

Accession Codes

CCDC 1575849, 2330988–2330991, and 2330993–2330994 contain the supplementary crystallographic data for this paper. These data can be obtained free of charge via www.ccdc.cam.ac.uk/data_request/cif, or by emailing data_request@ccdc.cam.ac.uk, or by contacting The Cambridge Crystallographic Data Centre, 12 Union Road, Cambridge CB2 1EZ, UK; fax: +44 1223 336033.

AUTHOR INFORMATION

Corresponding Author

Nikolaus Korber − *Institute of Inorganic Chemistry, University of Regensburg, 93053 Regensburg, Germany;* orcid.org/0000-0002-1880-8126; Email: nikolaus.korber@chemie.uni-regensburg.de

Authors

Stefanie Gärtner − *Institute of Inorganic Chemistry, University of Regensburg, 93053 Regensburg, Germany;* orcid.org/0000-0002-1382-344X

Michael Witzmann − *Institute of Inorganic Chemistry, University of Regensburg, 93053 Regensburg, Germany*

Corinna Lorenz-Fuchs − *Institute of Inorganic Chemistry, University of Regensburg, 93053 Regensburg, Germany*

Ruth M. Gschwind − *Institute of Organic Chemistry, University of Regensburg, 93053 Regensburg, Germany*

Complete contact information is available at: https://pubs.acs.org/10.1021/acs.inorgchem.4c01817

Funding

The authors gratefully acknowledge financial support from the German Science Foundation (DFG) (KO 1857/10-1 and GS 13/5-1).

Notes

The authors declare no competing financial interest.

ACKNOWLEDGMENTS

Special thanks to Dr. Franziska Fendt and Dr. Susanne M. Tiefenthaler for the preparation and data collection of SCXRD data for compounds **6** and **7**, respectively.

REFERENCES

(1) Joannis, A. C. Action du sodammonium et du potassammonium sur quelques méteaux. *C. R. Acad. Sci.* **1891**, *29*, n/a.

(2) Zintl, E.; Dallenkopf, W. Über den Gitterbau von NaTl und seine Beziehung zu den Strukturen des Typus des β -Messings. *Z. Phys. Chem. B* **1932**, *16*, 195–205.

(3) Zintl, E.; Goubean, J.; Dullenkopf, W. Salzartige Verbindungen und intermetallische Phasen des Natriums in flüssigem Ammoniak. *Z. Phys. Chem. A* **1931**, *154*, 1–46.

(4) Diehl, L.; Khodadadeh, K.; Kummer, D.; Strähle, J. Zintl's "Polyanionic Salts": Synthesis of the Crystalline Compounds $[Na_4\cdot 7en]Sn_9$, $[Na_4\cdot 5en]Ge_9$ and $[Na_3\cdot 4en]Sb_7$. The Crystal Structure of $[Na_4\cdot 7en]Sn_9$. *Z. Naturforsch. B* **1976**, *31*, 522–524.

(5) Corbett, J. D.; Edwards, P. A. Stable homopolyatomic anions: the crystal structures of salts of the anions pentaplumbide(2−) and enneastannide(4−). *Chem. Commun.* **1975**, 984–985.

(6) Corbett, J. D. Polyatomic Zintl Anions of the post-transition elements. *Chem. Rev.* **1985**, *85*, 383–397.

(7) Gärtner, S.; Korber, N. *Zintl Ions: Principles and Recent Developments* **2011**, *140*, 25–57.

(8) Scharfe, S.; Kraus, F.; Stegmaier, S.; Schier, A.; Fässler, T. F. Zintl Ions, Cage Compounds, and Intermetalloid Clusters of Group 14 and Group 15 Elements. *Angew. Chem., Int. Ed.* **2011**, *50*, 3630–3670.

(9) Fässler, T. F. The renaissance of homoatomic nine-atom polyhedra of the heavier carbon-group elements Si-Pb. *Coord. Chem. Rev.* **2001**, *215*, 347–377.

(10) Pan, F. X.; Weinert, B.; Dehnen, S. Binary Zintl Anions Involving Group 13–15 (Semi-)Metal Atoms, and the Relationship of Their Structures to Electron Count. *50th Anniversary of Electron Counting Paradigms for Polyhedral Molecules: Bonding in Clusters, Intermetallics and Intermetalloids* **2021**, *188*, 103–148.

(11) Corbett, J. D. Polyanionic Clusters and Networks of the Early p-Element Metals in the Solid State: Beyond the Zintl Boundary. *Angew. Chem., Int. Ed.* **2000**, *39*, 670−690.
(12) Ahlrichs, R.; Fenske, D.; Fromm, K.; Krautscheid, H.; Krautscheid, U.; Treutler, O. Zintl Anions as Starting Compounds for the Synthesis of Polynuclear Transition Metal Complexes. *Chem. - Eur. J.* **1996**, *2*, 238−244.
(13) Goicoechea, J. M. In *Clusters - Contemporary Insight in Structure and Bonding*; Springer, 2017; Vol. *174*, pp 63−97.
(14) Turbervill, R. S. P.; Goicoechea, J. M. From Clusters to Unorthodox Pnictogen Sources: Solution-Phase Reactivity of $[E_7]^{3-}$ (E = P-Sb) Anions. *Chem. Rev.* **2014**, *114*, 10807−10828.
(15) Sevov, S. C.; Goicoechea, J. M. Chemistry of Deltahedral Zintl Ions. *Organometallics* **2006**, *25*, 5678−5699.
(16) McGrady, J. E.; Weigend, F.; Dehnen, S. Electronic structure and bonding in endohedral Zintl clusters. *Chem. Soc. Rev.* **2022**, *51*, 628−649.
(17) Fässler, T. F. *Zintl Ions: Principles and Recent Developments* **2011**, *140*, 91−131.
(18) Liu, C.; Sun, Z. M. Recent advances in structural chemistry of Group 14 Zintl ions. *Coord. Chem. Rev.* **2019**, *382*, 32−56.
(19) Pan, F.; Guggolz, L.; Dehnen, S. Cluster Chemistry with (*Pseudo*-)Tetrahedra Involving Group 13−15 (Semi-)Metal Atoms. *CCS Chem.* **2022**, *4*, 809−824.
(20) Wilson, R. J.; Weinert, B.; Dehnen, S. Recent developments in Zintl cluster chemistry. *Dalton Trans.* **2018**, *47*, 14861−14869.
(21) von Schnering, H. G.; Schwarz, M.; Nesper, R. Rote, transparente Alkalimetallsilicide mit Si_4 Tetraedern. *Angew. Chem.* **1986**, *98*, 558−559.
(22) Busmann, E. Das Verhalten der Alkalimetalle zu Halbmetallen. X. Die Kristallstrukturen von KSi, RbSi, KGe, RbGe und CsGe. *Z. Anorg. Allg. Chem.* **1961**, *313*, 90−106.
(23) Goebel, T.; Prots, Y.; Haarmann, F. Refinement of the crystal structure of tetrasodium tetrasilicide, Na_4Si_4. *Z. Kristallogr. NCS* **2008**, *223*, 187−188.
(24) von Schnering, H. G.; Schwarz, M.; Chang, J. H.; Peters, K.; Peters, E. M.; Nesper, R. Refinement of the crystal structures of the tetrahedrotetrasilicides K_4Si_4, Rb_4Si_4 and Cs_4Si_4. *Z. Kristallogr. NCS* **2005**, *220*, 525−527.
(25) von Schnering, H. G.; Llanos, J.; Chang, J. H.; Peters, K.; Peters, E. M.; Nesper, R. Refinement of the crystal structures of the tetrahedro-tetragermanides K_4Ge_4, Rb_4Ge_4 and Cs_4Ge_4. *Z. Kristallogr. NCS* **2005**, *220*, 324−326.
(26) Grin, Y.; Baitinger, M.; Kniep, R.; von Schnering, H. G. Redetermination of the crystal structure of tetrasodium tetrahedro-tetrastannide, Na_4Sn_4 and tetrapotassium tetrahedro-tetrastannide, K_4Sn_4. *Z. Kristallogr. NCS* **1999**, *214*, 453−454.
(27) Baitinger, M.; Grin, Yu.; Kniep, R.; von Schnering, H. G. Crystal structure of tetrarubidium tetrahedro-tetrastannide, Rb_4Sn_4 and of tetracaesium tetrahedro-tetrastannide, Cs_4Sn_4. *Z. Kristallogr. NCS* **1999**, *214*, 457−458.
(28) Baitinger, M.; Peters, K.; Somer, M.; Carrillo-Cabrera, W.; Grin, Yu.; Kniep, R.; Schnering, H. G. v. Crystal structure of tetrarubidium tetrahedro-tetraplumbide, Rb_4Pb_4 and of tetracesium tetrahedro-tetraplumbide, Cs_4Pb_4. *Z. Kristallogr. NCS* **1999**, *214*, 455−456.
(29) Kliche, G.; von Schnering, H. G.; Schwarz, M. The Internal Vibrations of the Tetrahetero-Tetrahedrane Anions Ge_4^{4-}, Sn_4^{4-}, and Pb_4^{4-}. *Z. Anorg. Allg. Chem.* **1992**, *608*, 131−134.
(30) Ponou, S.; Fässler, T. F. Crystal Growth and Structure Refinement of K_4Ge_9. *Z. Anorg. Allg. Chem.* **2007**, *633*, 393−397.
(31) Guloy, A. M.; Tang, Z.; Ramlau, R.; Böhme, B.; Baitinger, M.; Grin, Y. Synthesis of the Clathrate-II $K_{8.6(4)}Ge_{136}$ by Oxidation of K_4Ge_9 in an Ionic Liquid. *Eur. J. Inorg. Chem.* **2009**, *2009*, 2455−2458.
(32) Hoch, C.; Wendorff, M.; Röhr, C. Synthesis and crystal structure of the tetrelides $A_{12}M_{17}$ (A = Na, K, Rb, Cs; M = Si, Ge, Sn) and A_4Pb_9 (A = K, Rb). *J. Alloys Compd.* **2003**, *361*, 206−221.
(33) Hoch, C.; Wendorff, M.; Röhr, C. Tetrapotassium nonastannide, K_4Sn_9. *Acta Crystallogr., Sect. C* **2002**, *58*, i45−i46.
(34) Queneau, V.; Todorov, E.; Sevov, S. C. Synthesis and structure of isolated silicon clusters of nine atoms. *J. Am. Chem. Soc.* **1998**, *120*, 3263−3264.
(35) Lorenz, C.; Gärtner, S.; Korber, N. Si_4^{4-} in Solution - First Solvate Crystal Structure of the Ligand-free Tetrasilicide Tetraanion in $Rb_{1.2}K_{2.8}Si_4$ $7NH_3$. *Z. Anorg. Allg. Chem.* **2017**, *643*, 141−145.
(36) Neumeier, M.; Fendt, F.; Gärtner, S.; Koch, C.; Gärtner, T.; Korber, N.; Gschwind, R. M. Detection of the Elusive Highly Charged Zintl Ions Si_4^{4-} and Sn_4^{4-} in Liquid Ammonia by NMR Spectroscopy. *Angew. Chem., Int. Ed.* **2013**, *52*, 4483−4486.
(37) Joseph, S.; Suchentrunk, C.; Korber, N. Dissolving Silicides: Syntheses and Crystal Structures of New Ammoniates Containing Si_5^{2-} and Si_9^{4-} Polyanions and the Role of Ammonia of Crystallisation. *Z. Naturforsch. B* **2010**, *65*, 1059−1065.
(38) Joseph, S.; Suchentrunk, C.; Kraus, F.; Korber, N. Si_9^{4-} Anions in Solution - Structures of the Solvates $Rb_4Si_9{\cdot}4.75NH_3$ and [Rb(18-crown-6)]$Rb_3Si_9{\cdot}4NH_3$, and Chemical Bonding in Si_9^{4-}. *Eur. J. Inorg. Chem.* **2009**, *2009*, 4641−4647.
(39) Hoch, C.; Wendorff, M.; Röhr, C. New Binary Alkaline Metal Stannides $A_{52}Sn_{82}$ (A = K, Cs) with Sn_4^{4-}-Zintl and Sn_9^{4-}-Cluster Anions. *Z. Anorg. Allg. Chem.* **2003**, *629*, 2391−2397.
(40) von Schnering, H. G.; Baitinger, M.; Bolle, U.; Carrillo-Cabrera, W.; Curda, J.; Grin, Y.; Heinemann, F.; Llanos, J.; Peters, K.; Schmeding, A.; Somer, M. Binary alkali metal compounds with the Zintl anions $[Ge9]^{4-}$ and $[Sn_9]^{4-}$. *Z. Anorg. Allg. Chem.* **1997**, *623*, 1037−1039.
(41) Lehmann, B.; Röhr, C. Crystal chemistry of alkali nona-stannid cluster compounds: Novelties from binary and novel ternary Ga-containing phases. *Z. Kristallogr. Suppl.* **2019**, *39*, 100.
(42) Meyer, T.; Hönle, W.; von Schnering, H. G. Chemistry and Structural Chemistry of Phosphides and Polyphosphides. 44. Tricesium Heptaphosphide Cs_3P_7: Preparation, Structure and Properties. *Z. Anorg. Allg. Chem.* **1987**, *552*, 69−80.
(43) Santandrea, R. P.; Mensing, C.; von Schnering, H. G. The sublimation and thermodynamic properties of the alkali metal phosphides Na_3P_7(s), K_3P_7(s), Rb_3P_7(s) and Cs_3P_7(s). *Thermochim. Acta* **1986**, *98*, 301−311.
(44) Emmerling, F.; Röhr, C. Alkaline Metal Arsenides A_3As_7 and AAs (A = K, Rb, Cs). Preparation, Crystal Structure, Vibrational Spectroscopy. *Z. Naturforsch. B* **2002**, *57*, 963−975.
(45) Hönle, W.; Buresch, J.; Peters, K.; Chang, J. H.; von Schnering, H. G. Crystal structure of the low-temperature modification of trisodium heptaarsenide, LT-Na_3As_7. *Z. Kristallogr. NCS* **2002**, *217*, 487−488.
(46) Hirschle, C.; Röhr, C. Synthesis and Crystal Structure of the known Zintl Phases Cs_3Sb_7 and Cs_4Sb_2. *Z. Anorg. Allg. Chem.* **2000**, *626*, 1992−1998.
(47) Dorn, F. W.; Klemm, W. Das Verhalten der Alkalimetalle zu Halbemetallen. V. Die Systeme des Antimons mit Kalium, Rubidium und Cäsium. *Z. Anorg. Allg. Chem.* **1961**, *309*, 189−203.
(48) von Schnering, H. G.; Somer, M.; Kliche, G.; Hönle, W.; Meyer, T.; Wolf, J.; Ohse, L.; Kempa, P. B. Chemistry and Structural Chemistry of Phosphides and Polyphosphides. 53. Preparation, Properties, and Vibrational Spectra of the Cage Anions P_{11}^{3-} and As_{11}^{3-}. *Z. Anorg. Allg. Chem.* **1991**, *601*, 13−30.
(49) Hönle, W.; Meyer, T.; Mensing, C.; von Schnering, H. G. X-ray Studies on Plastic-Crystalline Rb_3P_7, Cs_3P_{11} and $Cs_3(P_7)_{0.67}(P_{11})_{0.33}$. *Z. Kristallogr.* **1985**, *170*, 78−79.
(50) Wichelhaus, W.; von Schnering, H. G. Chemistry and Structural Chemistry of Phosphides and Polyphosphides. 6. Na_3P_{11}, Phosphide with isolated P_{11}^{3-} Groups. *Naturwissenschaften* **1973**, *60*, 104.
(51) von Schnering, H. G.; Meyer, T.; Hönle, W.; Schmettow, W.; Hinze, U.; Bauhofer, W.; Kliche, G. Chemistry and structural chemistry of phosphides and polyphosphides. 46. Tetrarubidiumhexaphosphide and tetracesiumhexaphosphide - Preparation, structure, and properties of Rb_4P_6 and Cs_4P_6. *Z. Anorg. Allg. Chem.* **1987**, *553*, 261−279.

https://doi.org/10.1021/acs.inorgchem.4c01817
Inorg. Chem. XXXX, XXX, XXX−XXX

(52) W, S.; Lipka, A.; G, v. S. H. Chemistry and structural chemistry of phosphides and polyphosphides. 10. Rb_4P_6, a phosphide with planar 6-membered phosphorus rings. *Angew. Chem., Int. Ed.* **1974**, *13*, 345.
(53) Hönle, W.; Krogull, G.; Peters, K.; von Schnering, H. G. Crystal structure of tetrarubidium cyclo-hexaarsenide(4-), Rb_4As_6 and of tetracesium cyclo-hexaarsenide(4-), Cs_4As_6. *Z. Kristallogr. NCS* **1999**, *214*, 17−18.
(54) Kraus, F.; Hanauer, T.; Korber, N. Nature of the chemical bond in polypnictides: The lone pair aromatic anions $P_4^{(2-)}$ and $As_4^{(2-)}$. *Inorg. Chem.* **2006**, *45*, 1117−1123.
(55) Gärtner, S.; Korber, N. In *Comprehensive Inorganic Chemistry II*, 2nd ed.; Reedijk, J., Poeppelmeier, K., Eds.; Elsevier: Amsterdam, 2013; pp 251−267.
(56) Lorenz, C.; Hastreiter, F.; Hioe, J.; Lokesh, N.; Gärtner, S.; Korber, N.; Gschwind, R. M. The Structure of HSi_9^{3-} in the Solid State and Its Unexpected Highly Dynamic Behavior in Solution. *Angew. Chem., Int. Ed.* **2018**, *57*, 12956−12960.
(57) Hastreiter, F.; Lorenz, C.; Hioe, J.; Gärtner, S.; Lokesh, N.; Korber, N.; Gschwind, R. M. Elusive Zintl Ions μ-HSi_4^{3-} and Si_5^{2-} in Liquid Ammonia: Protonation States, Sites, and Bonding Situation Evaluated by NMR and Theory. *Angew. Chem., Int. Ed.* **2019**, *58*, 3133−3137.
(58) Streitferdt, V.; Tiefenthaler, S. M.; Shenderovich, I. G.; Gärtner, S.; Korber, N.; Gschwind, R. M. NMR-Spectroscopic Detection of an Elusive Protonated and Coinage Metalated Silicide $[NHC^{Dipp}Cu(\eta^4\text{-}Si_9)H]^{2-}$ in Solution. *Eur. J. Inorg. Chem.* **2021**, *2021*, 3684−3690.
(59) Tiefenthaler, S. M.; Streitferdt, V.; Baumann, J.; Gärtner, S.; Gschwind, R. M.; Korber, N. On the Reactivity of $NHC^{tBu}AuCl$ towards $Rb_6Cs_6Si_{17}$: The First Gold-Silicon Cluster $[(NHC^{tBu}Au)_6(\eta^2\text{-}Si_4)]Cl_2{\cdot}7NH_3$ and an Imide Capped Gold Triangle $(NHC^{tBu}Au)_3NHCl$. *Z. Anorg. Allg. Chem.* **2020**, *646*, 1595−1602.
(60) Kraus, F. I.; Hanauer, T.; Korber, N. Chemical bond in the Cyclic Anions P_6^{4-} and As_6^{4-}: Synthesis, Crystal Structure, and Electron Localization Function of $\{Rb[18]crown\text{-}6)\}_2Rb_2As_6$ 6 NH_3. *Angew. Chem., Int. Ed.* **2005**, *44*, 7200−7204.
(61) Fendt, F.; Koch, C.; Neumeier, M.; Gärtner, S.; Gschwind, R. M.; Korber, N. Stability and Conversion of Tin Zintl Anions in Liquid Ammonia Investigated by NMR Spectroscopy. *Chem. - Eur. J.* **2015**, *21*, 14539−14544.
(62) Graubner, T.; Woidy, P.; Bär, S. A.; Karttunen, A. J.; Kraus, F. Uranium Chemistry in liquid Ammonia: Compounds obtained by adventitious Presence of Moisture or Air. *Eur. J. Inorg. Chem.* **2024**, *27*, e202300752.
(63) Sheldrick, G. M. SHELXT - Integrated space-group and crystal-structure determination. *Acta Cryst. A* **2015**, *71*, 3−8.
(64) Sheldrick, G. M. Crystal structure refinement with SHELXL. *Acta Cryst. C* **2015**, *71*, 3−8.
(65) Dolomanov, O. V.; Bourhis, L. J.; Gildea, R. J.; Howard, J. A. K.; Puschmann, H. OLEX2: a complete structure solution, refinement and analysis program. *J. Appl. Crystallogr.* **2009**, *42*, 339−341.
(66) Putz, H.; Putz, K. *Diamond - Crystal and Molecular Structure Visualization*, ver. 4.6; 2023.
(67) Somer, M.; Hönle, W.; von Schnering, H. G. Syntheses, Crystal-Structure and Vibrational-Spectra of Cs_3As_7 and $Cs_3(NH_3)$-As_7. *Z. Naturforsch. B* **1989**, *44*, 296−306.
(68) Lorenz, C.; Gärtner, S.; Korber, N. Ammoniates of Zintl Phases: Similarities and Differences of Binary Phases A_4E_4 and Their Corresponding Solvates. *Crystals* **2018**, *8*, 276−292.
(69) Benda, C. B.; Henneberger, T.; Klein, W.; Fässler, T. F. $[Si_4]^{4-}$ and $[Si_9]^{4-}$ Clusters Crystallized from Liquid Ammonia Solution − Synthesis and Characterization of $K_8[Si_4][Si_9]{\cdot}(NH_3)_{14.6}$. *Z. Anorg. Allg. Chem.* **2017**, *643*, 146−148.
(70) Hanauer, T.; Grothe, M.; Reil, M.; Korber, N. Syntheses and Crystal Structures of Four New Ammoniates with Heptaarsenide (As_7^{3-}) Anions. *Helv. Chim. Acta* **2005**, *88*, 950−961.
(71) Korber, N.; Fleischmann, A. Synthesis and crystal structure of $[Li(NH_3)_4]_4[Sn_9]{\cdot}NH_3$ and $[Li(NH3)_4]_4[Pb_9]{\cdot}NH_3$. *Dalton Trans.* **2001**, 383−385.
(72) Gärtner, S.; Korber, N. [Rb(18-crown-6)][Rb([2.2.2]-cryptand)]$Rb_2Sn_9{\cdot}5NH_3$. *Acta Crystallogr., Sect. E* **2011**, *67*, m613−m614.
(73) Wiesler, K.; Brandl, K.; Fleischmann, A.; Korber, N. Tetrahedral $[Tt_4]^{4-}$ Zintl Anions Through Solution Chemistry: Syntheses and Crystal Structures of the Ammoniates $Rb_4Sn_4{\cdot}2NH_3$, $Cs_4Sn_4{\cdot}2NH_3$, and $Rb_4Pb_4{\cdot}2NH_3$. *Z. Anorg. Allg. Chem.* **2009**, *635*, 508−512.
(74) Klein, W.; Benda, C. B.; Henneberger, T.; Witzel, B. J. L.; Fässler, T. F. Investigations on the Solubility of Sn_4-Cluster Compounds in Liquid Ammonia. *Z. Anorg. Allg. Chem.* **2021**, *647*, 2047−2054.
(75) Beekman, M.; Kauzlarich, S. M.; Doherty, L.; Nolas, G. S. Zintl Phases as Reactive Precursors for Synthesis of Novel Silicon and Germanium-Based Materials. *Materials* **2019**, *12*, 1139−1160.
(76) Veremchuk, I.; Beekman, M.; Antonyshyn, I.; Schnelle, W.; Baitinger, M.; Nolas, G. S.; Grin, Y. Binary Alkali-Metal Silicon Clathrates by Spark Plasma Sintering: Preparation and Characterization. *Materials* **2016**, *9*, 593−602.
(77) Müller-Buschbaum, P.; Thelakkat, M.; Fässler, T. F.; Stutzmann, M. Hybrid Photovoltaics - from Fundamentals towards Application. *Adv. Energy Mater.* **2017**, *7*, 1700248.
(78) Kauzlarich, S. M. Special Issue: Advances in Zintl Phases. *Materials* **2019**, *12*, 2554−2556.
(79) Kauzlarich, S. M. Zintl Phases: From Curiosities to Impactful Materials. *Chem. Mater.* **2023**, *35*, 7355−7362.
(80) Kysliak, O.; Schrenk, C.; Schnepf, A. The Largest Metalloid Group 14 Cluster, Ge18[Si(SiMe3)3]6: An Intermediate on the Way to Elemental Germanium. *Angew. Chem. Int. Ed* **2016**, *55*, 3216−3219.
(81) Karttunen, A. J.; Fässler, T. F.; Linnolahti, M.; Pakkanen, T. A. Two-, One-, and Zero-Dimensional Elemental Nanostructures Based on Ge_9-Clusters. *ChemPhys. Chem.* **2010**, *11*, 1944−1950.
(82) Jantke, L. A.; Karttunen, A. J.; Fässler, T. F. Chemi-Inspired Silicon Allotropes—Experimentally Accessible Si_9 Cages as Proposed Building Block for 1D Polymers, 2D Sheets, Single-Walled Nanotubes, and Nanoparticles. *Molecules* **2022**, *27*, 822−836.
(83) Nolan, B. M.; Henneberger, T.; Waibel, M.; Fässler, T. F.; Kauzlarich, S. M. Silicon Nanoparticles by the Oxidation of $[Si_4]^{4-}$- and $[Si_9]^{4-}$-Containing Zintl Phases and Their Corresponding Yield. *Inorg. Chem.* **2015**, *54*, 396−401.
(84) Guloy, A. M.; Ramlau, R.; Tang, Z.; Schnelle, W.; Baitinger, M.; Grin, Y. A guest-free germanium clathrate. *Nature* **2006**, *443*, 320−323.
(85) Armatas, G. S.; Kanatzidis, M. G. Mesostructured germanium with cubic pore symmetry. *Nature* **2006**, *441*, 1122−1125.
(86) Sun, D.; Riley, A. E.; Cadby, A. J.; Richman, E. K.; Korlann, S. D.; Tolbert, S. H. Hexagonal nanoporous germanium through surfactant-driven self-assembly of Zintl clusters. *Nature* **2006**, *441*, 1126−1130.
(87) Armatas, G. S.; Kanatzidis, M. G. Hexagonal Mesoporous Germanium. *Science* **2006**, *313*, 817−820.
(88) Auer, H.; Kohlmann, H. In situ Investigations on the Formation and Decomposition of $KSiH_3$ and $CsSiH_3$. *Z. Anorg. Allg. Chem.* **2017**, *643*, 945−951.
(89) Ugrinov, A.; Sevov, S. C. Rationally Functionalized Deltahedral Zintl Ions: Synthesis and Characterization of $[Ge_9 - ER_3]^{3-}$, $[R_3E - Ge_9 - ER_3]^{2-}$, and $[R_3E - Ge_9 - Ge_9 - ER_3]^{4-}$ (E = Ge, Sn; R = Me, Ph). *Chem. - Eur. J.* **2004**, *10*, 3727−3733.
(90) Baudler, M.; Winzek, P. Contributions to the Chemistry of Phosphorus. 241. On the Reaction of Diphosphane(4) with Liquid Ammonia and with Amines − a New Route to Polyphosphides and Hydrogen Polyphosphides. *Z. Anorg. Allg. Chem.* **1999**, *625*, 417−422.
(91) Baudler, M.; Glinka, K. Open-Chain Polyphosphorus Hydrides (Phosphines). *Chem. Rev.* **1994**, *94*, 1273−1297.

https://doi.org/10.1021/acs.inorgchem.4c01817
Inorg. Chem. XXXX, XXX, XXX−XXX

(92) Baudler, M.; Glinka, K. Contributions to the chemistry of phosphorus. 218. Monocyclic and polycyclic phosphanes. *Chem. Rev.* **1993**, *93*, 1623−1667.
(93) Baudler, M.; Faber, W.; Hahn, J. Contributions to the Chemistry of Phosphorus. 97. Preparation and Properties of Trimethyl-heptaphosphane(3), $P_7(CH_3)_3$. *Z. Anorg. Allg. Chem.* **1980**, *469*, 15−21.
(94) Kocak, F. S.; Downing, D. O.; Zavalij, P.; Lam, Y. F.; Vedernikov, A. N.; Eichhorn, B. Surprising Acid/Base and Ion-Sequestration Chemistry of Sn_9^{4-}: HSn_9^{3-}, $Ni@HSn_9^{3-}$, and the Sn_9^{3-} Ion Revisited. *J. Am. Chem. Soc.* **2012**, *134*, 9733−9740.
(95) Schiegerl, L. J.; Karttunen, A. J.; Tillmann, J.; Geier, S.; Raudaschl-Sieber, G.; Waibel, M.; Fässler, T. F. Charged Si_9 Clusters in Neat Solids and the Detection of $[H_2Si_9]^{2-}$ in Solution: A Combined NMR, Raman, Mass Spectrometric, and Quantum Chemical Investigation. *Angew. Chem., Int. Ed.* **2018**, *57*, 12950−12955.
(96) Lorenz, C.; Korber, N. Crystal Structure of the Protonated Germanide Cluster $[HGe_9]^{3-}$. *Crystals* **2018**, *8*, 374−383.
(97) Korber, N.; Daniels, J. Dicaesium Ethyltrimethylammonium Heptaphosphide−Ammonia (1/2). *Acta Crystallogr. C* **1996**, *52*, 2454−2457.
(98) Korber, N.; Daniels, J.; von Schnering, H. G. Directed Synthesis of Stable Hydrogen Polyphosphides: Preparation and Structural Characterization of HP_{11}^{2-} in $(NBnMe_3)_2HP_{11}$ and $(PBnPh_3)_2HP_{11}$ as Well as Its Comparison with the First "Naked" P_{11}^{3-} Ion in $(NEtMe_3)_3P_{11}$. *Angew. Chem., Int. Ed.* **1996**, *35*, 1107−1110.
(99) Korber, N.; von Schnering, H. G. $PPh_4^+H_2P_7^-$—the first stable hydrogen polyphosphide salt. *Chem. Commun.* **1995**, 1713−1714.
(100) Henneberger, T.; Klein, W.; Dums, J. V.; Fässler, T. F. $[(\mu_2\text{-}H)(\eta^2\text{-}Ge_4)ZnPh_2]^{3-}$, an edge-on protonated E_4 cluster establishing the first three-center two-electron Ge−H−Ge bond. *Chem. Commun.* **2018**, *54*, 12381−12384.
(101) Sichevych, O.; Akselrud, L.; Böhme, B.; Bobnar, M.; Baitinger, M.; Wagner, F. R.; Grin, Y. K_2BaSi_4: Zintl Concept in Position Space. *Z. Anorg. Allg. Chem.* **2023**, *649*, e202300116.
(102) Wiesner, A.; Steinhauer, S.; Beckers, H.; Müller, C.; Riedel, S. $[P_4H^+]$ $[Al(OTeF_5)_4^-$: protonation of white phosphorus with the Bronsted superacid $H[Al(OTeF_5)]_{4(solv)}$. *Chem. Sci.* **2018**, *9*, 7169.
(103) Wiesner, A.; Gries, T. W.; Steinhauer, S.; Beckers, H.; Riedel, S. Superacids Based on Pentafluoroorthotellurate Derivatives of Aluminum. *Angew. Chem., Int. Ed.* **2017**, *56*, 8263−8266.
(104) Somer, M.; Carrillo-Cabrera, W.; Peters, E. M.; Peters, K.; Kaupp, M.; von Schnering, H. G. The $[Sn_5]^{2-}$ Cluster Compound $[K\text{-}(2,2,2\text{-crypt})]_2Sn_5$ − Synthesis, Crystal Structure, Raman Spectrum, and Hierarchical Relationship to $CaIn_2$. *Z. Anorg. Allg. Chem.* **1999**, *625*, 37−42.
(105) Edwards, P. A.; Corbett, J. D. Stable homopolyatomic anions. Synthesis and crystal structures of salts containing the pentaplumbide(2-) and pentastannide(2-) anions. *Inorg. Chem.* **1977**, *16*, 903−907.
(106) Suchentrunk, C.; Korber, N. Ge_5^{2-} Zintl anions: synthesis and crystal structures of $[K([2.2.2]\text{-crypt})]_2Ge_5{\cdot}4NH_3$ and $[Rb([2.2.2]\text{-crypt})]_2Ge_5{\cdot}4NH_3$. *New J. Chem.* **2006**, *30*, 1737−1739.
(107) von Schnering, H. G.; Somer, M.; Kaupp, M.; Carrillo-Cabrera, W.; Baitinger, M.; Schmeding, A.; Grin, Y. The Cluster Anion Si_9^{4-}. *Angew. Chem., Int. Ed.* **1998**, *37*, 2359−2361.
(108) Goicoechea, J. M.; Sevov, S. C. Naked Deltahedral Silicon Clusters in Solution: Synthesis and Characterization of Si_9^{3-} and Si_5^{2-}. *J. Am. Chem. Soc.* **2004**, *126*, 6860−6861.
(109) Cisar, A.; Corbett, J. D. Polybismuth anions. Synthesis and crystal structure of a salt of the tetrabismuthide(2-) ion, Bi_4^{2-}. A basis for the interpretation of the structure of some complex intermetallic phases. *Inorg. Chem.* **1977**, *16*, 2482−2487.
(110) Critchlow, S. C.; Corbett, J. D. Homopolyatomic anions of the post transition elements. Synthesis and structure of potassium-crypt salts of the tetraantimonide(2-) and heptaantimonide(3-) anions, Sb_4^{2-} and Sb_7^{3-}. *Inorg. Chem.* **1984**, *23*, 770−774.
(111) Hanauer, T.; Kraus, F.; Reil, M.; Korber, N. Isolated cyclo-Tetraarsendiide Anions: Synthesis and Crystal Structures of Bis-(tetraamminelithium) tetraarsenide $[Li(NH_3)_4]_2As_4$, Bis-(pentaamminesodium) tetraarsenide − ammonia (1/3) $[Na(NH_3)_5]_2As_4 \cdot 3NH_3$ and Bis[(4,7,13,16,21,24-hexaoxa-1,10-diazabicyclo [8.8.8]hexacosan)(cesium, rubidium)] tetraarsenide − ammonia (1/2) $[Cs_{0.35}Rb_{0.65}(2,2,2\text{-crypt})]_2As_4 \cdot 2NH_3$. *Monatsh. Chem.* **2006**, *137*, 147−156.
(112) Kraus, F.; Korber, N. The Chemical Bond in Polyphosphides: Crystal Structures, the Electron Localization Function, and a New View of Aromaticity in P_4^{2-} and P_5^-. *Chem. - Eur. J.* **2005**, *11*, 5945−5959.
(113) Kraus, F.; Aschenbrenner, J. C.; Korber, N. P_4^{2-}: A 6π Aromatic Polyphosphide in Dicesium Cyclotetraphosphide−Ammonia (1/2). *Angew. Chem., Int. Ed.* **2003**, *42*, 4030−4033.
(114) Janesch, M.; Schwinghammer, V. F.; Shenderovich, I. G.; Gärtner, S. Synthesis and characterization of ternary trielides Na_7KTr_4 [Tr = In or Tl] including $[Tr_4]^{8-}$ Tetrahedra. *Z. Anorg. Allg. Chem.* **2023**, *649*, e202300112.
(115) Schwinghammer, V. F.; Janesch, M.; Korber, N.; Gartner, S. Na_7RbTl_4 − A New Ternary Zintl Phase Containing $[Tl_4]^{8-}$ Tetrahedra. *Z. Anorg. Allg. Chem.* **2022**, *648*, e202200332.
(116) Schwinghammer, V. F.; Gärtner, S. $[Tl_7]^{7-}$ Clusters in Mixed Alkali Metal Thallides $Cs_{7.29}K_{5.71}Tl_{13}$ and $Cs_{3.45}K_{3.55}Tl_7$. *Inorg. Chem.* **2024**, DOI: 10.1021/acs.inorgchem.3c04034.
(117) Hanauer, T.; Aschenbrenner, J. C.; Korber, N. Dimers of Heptapnictide Anions: As_{14}^{4-} and P_{14}^{4-} in the Crystal Structures of $[Rb(18\text{-crown-}6)]_4As_{14}{\cdot}6NH_3$ and $[Li(NH_3)_4]_4P_{14}{\cdot}NH_3$. *Inorg. Chem.* **2006**, *45*, 6723−6727.
(118) Suchentrunk, C.; Daniels, J.; Somer, M.; Carrillo-Cabrera, W.; Korber, N. Synthesis And Crystal Structures Of The Polygermanide Ammoniates $K_4Ge_9 \cdot 9\ NH_3$, $Rb_4Ge_9 \cdot 5\ NH_3$ And $Cs_6Ge_{18} \cdot 4\ NH_3$. *Z. Naturforsch. B* **2005**, *60*, 277−283.
(119) Meier, M.; Faupel, V.; Korber, N. First Polymeric Polyphosphide via Solution Chemistry − Synthesis and Crystal Structure of CsP_7. *Z. Anorg. Allg. Chem.* **2014**, *640*, 2659−2662.

https://doi.org/10.1021/acs.inorgchem.4c01817
Inorg. Chem. XXXX, XXX, XXX−XXX